HHS Public Access

Author manuscript

Biochim Biophys Acta. Author manuscript; available in PMC 2016 November 01.

Published in final edited form as:

Biochim Biophys Acta. 2016 November ; 1862(11): 2023–2033. doi:10.1016/j.bbadis.2016.08.005.

Disruption of calpain reduces lipotoxicity-induced cardiac injury by preventing endoplasmic reticulum stress

Shengcun Li[a], **Lulu Zhang**[a], **Rui Ni**[a,e,g], **Ting Cao**[a], **Dong Zheng**[a,e,f], **Sidong Xiong**[a], **Peter A. Greer**[b,c], **Guo-Chang Fan**[d], and **Tianqing Peng**[a,e,f,g,*]

Tianqing Peng: tpeng2@uwo.ca

[a]Institutes of Biology and Medical Sciences, Soochow University, Suzhou, Jiangsu Province 215123, China

[b]Division of Cancer Biology and Genetics, Queen's University Cancer Research Institute, Kingston, Ontario K7L 3N6, Canada

[c]Department of Pathology and Molecular Medicine, Queen's University, Kingston, Ontario K7L 3N6, Canada

[d]Department of Pharmacology and Cell Biophysics, University of Cincinnati College of Medicine, Cincinnati, OH 45267, USA

[e]Critical Illness Research, Lawson Health Research Institute, Western University, London, Ontario N6A 4G5, Canada

[f]Department of Medicine, Western University, London, Ontario N6A 4G5, Canada

[g]Department of Pathology and Laboratory Medicine, Western University, London, Ontario N6A 4G5, Canada

Abstract

Diabetes and obesity are prevalent in westernized countries. In both conditions, excessive fatty acid uptake by cardiomyocytes induces cardiac lipotoxicity, an important mechanism contributing to diabetic cardiomyopathy. This study investigated the effect of calpain disruption on cardiac lipotoxicity. Cardiac-specific *capns1* knockout mice and their wild-type littermates (male, age of 4 weeks) were fed a high fat diet (HFD) or normal diet for 20 weeks. HFD increased body weight, altered blood lipid profiles and impaired glucose tolerance comparably in both *capns1* knockout mice and their wild-type littermates. Calpain activity, cardiomyocyte cross-sectional areas, collagen deposition and triglyceride were significantly increased in HFD-fed mouse hearts, and these were accompanied by myocardial dysfunction and up-regulation of hypertrophic and fibrotic collagen genes as well as pro-inflammatory cytokines. These effects of HFD were attenuated by disruption of calpain in *capns1* knockout mice. Mechanistically, deletion of *capns1* in HFD-fed mouse hearts and disruption of calpain with calpain inhibitor-III, silencing of *capn1*, or deletion of

*Corresponding author at: Critical Illness Research, Lawson Health Research Institute, VRL 6th Floor, A6-140, 800 Commissioners Road, London, Ontario N6A 4G5, Canada.

Transparency document: The Transparency document associated with this article can be found, in online version.

Appendix A. Supplementary data: Supplementary data to this article can be found online at http://dx.doi.org/10.1016/j.bbadis.2016.08.005.

capns1 in palmitate-stimulated cardiomyocytes prevented endoplasmic reticulum stress, apoptosis, cleavage of caspase-12 and junctophilin-2, and pro-inflammatory cytokine expression. Pharmacological inhibition of endoplasmic reticulum stress diminished palmitate-induced apoptosis and pro-inflammatory cytokine expression in cardiomyocytes. In summary, disruption of calpain prevents lipotoxicity-induced apoptosis in cardiomyocytes and cardiac injury in mice fed a HFD. The role of calpain is mediated, at least partially, through endoplasmic reticulum stress. Thus, calpain/endoplasmic reticulum stress may represent a new mechanism and potential therapeutic targets for cardiac lipotoxicity.

Keywords

Calpain; Cardiomyocytes; Lipotoxicity; Endoplasmic reticulum stress

1. Introduction

Diabetes and obesity are prevalent in westernized countries. In both conditions, excessive fatty acid uptake by cardiomyocytes may alter cellular structures and activate downstream pathways in the heart resulting in cardiomyocyte apoptosis and/or impaired insulin signaling followed by decreased glucose use and myocardial dysfunction, a condition described as cardiac lipotoxicity [1–3], eventually leading to adverse myocardial remodeling and heart failure. In addition to glucotoxicity, lipotoxicity is also an important mechanism contributing to diabetic cardiomyopathy [3], a condition independent of coronary artery disease and hypertension. However, the underlying mechanisms responsible for cardiac lipotoxicity remain partially understood.

Calpains are Ca^{2+}-dependent intracellular proteases [4]. Amongst 15 family members, two of the best characterized calpain species are calpain-1 and calpain-2. These isoforms are heterodimers consisting of ~80 kDa catalytic subunits, encoded by the capn1 and capn2 genes, respectively, and a ~30 kDa small regulatory subunit encoded by *capns1* (also known as *capn4*). The small regulatory subunit is essential for the stability and catalytic activity of calpain-1 and calpain-2. Thus, deletion of *capns1* in mice abolished calpain-1 and calpain-2 activity [5]. Calpain-1 and calpain-2 activities are also tightly controlled by the endogenous inhibitor calpastatin. Calpain activation has been implicated in myocardial remodeling and heart failure [6]. We have recently demonstrated that calpain activation mediates apoptosis in high glucose-stimulated cardiomyocytes [7] and genetic inhibition of calpain reduces adverse cardiac remodeling and myocardial dysfunction in hyperglycemic mice [5], indicating a critical role of calpain in cardiac glucotoxicity. However, it remains to be determined whether calpain plays a role in cardiac lipotoxicity.

Endoplasmic reticulum (ER) stress is induced by accumulation of unfold proteins, resulting from oxidative stress, ischemia, disturbance of calcium homeostasis, and over-expression of normal and/or incorrectly folded proteins [8]. ER stress-associated unfolded protein response activates ER transmembrane sensors including protein kinase-like ER kinase, inositol-requiring kinase 1, and activating transcription factor 6. These tree branches of ER trans-membrane sensors initiate adaptive response through phosphorylation of eukaryotic

translation initiation factor 2α, transcription factor ATF4 translation, X-Box Binding Protein 1 splicing, and finally the induction of the unfolded protein response related genes, including chaperones glucose-regulated protein-78 (GRP78) and -94 (GRP94), and C/EBP homologous protein (CHOP). If ER stress is prolonged or overwhelming, however, it can induce apoptotic cell death through CHOP and/or other pathways. Recent animal and human studies have demonstrated that ER stress is implicated in the pathophysiology of various cardiovascular diseases [9,10]. ER stress is induced and has been implicated in cardiac lipotoxicity [11–13]. We reported that calpain activation induces ER stress in cardiomyocytes following ischemia/reperfusion [14]. However, it remains to be determined whether calpain regulates ER stress in cardiac lipotoxicity.

In this study, we analyzed the impact of calpain disruption on ER stress, myocardial hypertrophy, fibrosis and pro-inflammatory response in a mouse model of high fat diet (HFD)-induced cardiac lipotoxicity. We further investigated the direct relationship between calpain, ER stress, and apoptosis and pro-inflammatory response in palmitate-stimulated cardiomyocytes.

2. Materials and methods

2.1. Animals

This investigation conforms to the Guide for the Care and Use of Laboratory Animals published by the US National Institutes of Health (NIH Publication No. 85-23). All experimental procedures were approved by the Animal Use Subcommittee at the Soochow University, China. Breeding pairs of C57BL/6 mice were purchased from the Jackson Laboratory. Mice with cardiomyocyte-specific disruption of *capns1* (*capns1*-ko) were generated by breeding mice bearing the targeted $Capn4^{PZ}$ allele containing *loxP* sites flanking essential coding exons and mice with cardiomyocyte-specific expression of Cre recombinase under the control of alpha-myosin heavy chain as we recently described [5]. All of the mice used in this study, including controls, were littermates of the same generation. A breeding program was implemented at Soochow University's animal care facilities.

2.2. Experimental protocol

Male *capns1-ko* mice and their wild-type littermates (mice bearing the targeted $Capn4^{PZ}$ allele containing *loxP* sites flanking essential coding exons) at age of 4 weeks were fed a high fat diet (HFD) or normal diet (ND) for 20 weeks. This HFD contains 26.2% of protein, 26.3% of carbohydrate and 34.9% of fat (% by weight) (Research Diets Inc., USA). The calculated caloric intake from these nutrients (% kcal) is 20%, 20% and 60%, respectively. At the end of each experiment, mice were anaesthetized with ketamine (100 mg/kg)/xylazine (5 mg/kg, i.p.) and blood was taken from anaesthetized mice via the cardiac puncture. Mice were then euthanized by cervical dislocation right away.

2.3. Blood pressure measurement

Blood pressure was measured using a tail-cuff method. Briefly, mice were gently restrained in a holder and warmed to 37 °C by a heating platform under the holder. Animals were acclimated in the environment for 5–10 min after occlusion cuffs and pulse transducers

(MRBP system, IITC Life Science, USA) were placed on the tail. The values of at least 10 readings for each mouse were used for blood pressure.

2.4. Intraperitoneal glucose tolerance

For intraperitoneal glucose tolerance test (IPGTT), 16-hour fasted mice were given a glucose load (2 g/kg, i.p.). Blood samples were taken from the tail vein at 0, 15, 30, 60, 120 min after glucose injection, and blood glucose was measured using a glucose meter (LifeScan, USA).

2.5. Blood lipid profiles

Blood samples were obtained in mice after 5-hour fasting. Total cholesterol (TC), triglyceride (TG), low-density lipoprotein cholesterol (LDL-C), and high-density lipoprotein cholesterol (HDL-C) were measured by using commercially available kits (Nanjing Jiancheng Bioengineering Institute, China) according to the manufacturer's instruction.

2.6. Echocardiography

Animals were lightly anaesthetized with inhalant isoflurane (1%) and imaged using a 40-MHz linear array transducer attached to a pre-clinical ultrasound system (Vevo 2100, FUJIFILM VisualSonics, Canada) with nominal in-plane spatial resolution of 40 μm (axial) × 80 μm (lateral). M-mode and 2-D parasternal short-axis scans (133 frames/s) at the level of the papillary muscles were used to assess changes in left ventricle (LV) end-systolic inner diameter, LV end-diastolic inner diameter, and fractional shortening (FS%) [15,16].

To assess diastolic function, we obtained apical four-chamber views of the left ventricle. The pulsed wave Doppler measurements of maximal early (E) and late (A) transmitral velocities in diastole were obtained in the apical view with a cursor at mitral valve inflow [16].

2.7. Mouse cardiomyocyte cultures

Neonatal mice (born within 2 days) were euthanized by decapitation and the neonatal cardiomyocytes were prepared and cultured according to methods we described previously [14].

Adult cardiomyocytes were isolated and cultured as we described previously [15].

2.8. Treatment of siRNA

Cholesterol-conjugated siRNAs for *capn1* and *capn2* were purchased from Guangzhou Ribobio Co., Ltd. (China). The sequences for *capn1* and *capn2* siRNA are as follows: 5′CCAGCTACCTTCTGGGTAA3′ (*capn1* siRNA) and 5′GGAGAAAGGTTCTCTGCTT3′ (*capn2* siRNA). A scrambled siRNA conjugated with cholesterol served as a control. Cardiomyocytes were incubated with siRNA (50 nmol/L) in normal culture medium. Cholesterol-conjugated siRNAs enter cardiomyocytes directly with an efficiency of more than 90% (data not shown).

2.9. Histological analyses

The total collagen content and cardiomyocyte cross-sectional areas were assessed as described in our recent report [5]. The content of collagen-1 and collagen-3 was determined by using the polarization microscopy after staining with Picro-sirius Red (Cedarlane Laboratories, Canada).

2.10. Calpain activity

Calpain activities were assessed in cultured cardiomyocytes and heart tissues using a fluorescence substrate N-succinyl-LLVY-AMC (Cedarlane Laboratories, Canada) as described previously [15].

2.11. Active caspase-3

Caspase-3 activity was measured in cultured cardiomyocytes and heart tissues using a caspase-3 fluorescence assay kit (Biomol Research Laboratories, USA) as described in our previous reports [5].

2.12. Measurement of cellular DNA fragmentation

Cardiomyocytes were pre-labelled with BrdU and then incubated with doxorubicin. DNA fragmentation was measured using a Cellular DNA Fragmentation ELISA kit (Roche Applied Science, Canada) according to the manufacturer's instructions.

2.13. Real-time reverse-transcriptase polymerase chain reaction (RT-PCR)

Real-time RT-PCR was performed to analyze mRNA expression for beta-myosin heavy chain (β-MHC), atrial natriuretic peptide (ANP), collagen-1 and -3, tumor necrosis factor-alpha (TNF-α), interleukin-1 beta (IL-1β) and GAPDH as described previously [16].

2.14. Western blot analysis

The protein levels of CAPN1, CAPN2, GRP78, CHOP, phosphorylated and total JNK1/2, junctophilin-2, caspase-12, SERCA2a, stromal interaction molecule 1 (STIM1) and GAPDH were determined by western blot analysis using respective specific antibodies (Cell Signaling, USA).

2.15. Statistical analysis

All data were presented as mean ± SD. Two-way ANOVA followed by Newman-Keuls tests were performed for multi-group comparisons. A student's *t*-test was used for comparison between 2 groups. A value of $P < 0.05$ was considered statistically significant.

3. Results

3.1. HFD induces metabolic abnormity in mice and increases calpain activity in the heart

To investigate the role of calpain in cardiac lipotoxicity, we fed *capns1*-ko mice and their wild-type littermates a HFD or ND as a control. Twenty weeks after feeding with a HFD, mice exhibited increased body weight, hyperlipidemia (elevations of TC, TG, LDL and HDLinblood) and impairment of glucose tolerance as compared to ND-fed animals

(Supplemental Tables 1 and 2, Fig. 1a and b), indicative of obesity and type-2 diabetes. Deficiency of *capns1* did not change these metabolic parameters. The blood pressure remained similar between 4 groups (Supplemental Table 3). These results suggest that cardiomyocyte-specific deletion of *capns1* does not affect systemic metabolism in *capns1*-ko mice.

As compared to ND-fed mice, HFD significantly increased the content of triglyceride (Fig. 1c) in mouse hearts. HFD up-regulated the mRNA levels of CD36 but not other glucose and fatty acids metabolic gene such as GLUT4, ACC1 and PGC1α in mouse hearts (Supplemental Fig. 1a–d). HFD induced calpain activation (Supplemental Fig. 2) in hearts. The up-regulation of calpain activity was not due to alterations in calpain and calpastatin expression because the protein levels of CAPN1, CAPN2 and calpastatin were not significantly altered in heart tissues from mice fed a HFD versus ND (data not shown). There was no death during feeding a HFD and ND.

3.2. Deficiency of capns1 protects myocardial function in mice fed a HFD

Consistent with other reports in cardiac lipotoxicity [17], myocardial function was compromised in mice fed a HFD. As shown in Fig. 1d–h and Supplemental Table 4, wild-type mice fed a HFD displayed a decrease in FS% and EF%, indicative of systolic dysfunction and a reduction in E/A ratio, indicative of diastolic dysfunction, relative to mice fed a ND. In contrast, both systolic and diastolic functions were relatively preserved in *capns1*-ko mice fed a HFD compared with ND. This suggests that deletion of *capns1* prevents myocardial dysfunction in mice fed a HFD.

3.3. Deletion of capns1 reduces myocardial hypertrophy in mice fed a HFD

Twenty weeks after feeding with a HFD, the ratio of heart weight to body weight or tibia length was increased as compared to ND-fed mice (Fig. 2a and Supplemental Table 1). Histological analysis of cardiomyocyte cross-sectional areas in wild-type mice revealed an increase in cardiomyocyte size, indicative of cardiomyocyte hypertrophy. However, cardiomyocyte sizes were not increased in *capns1-ko* mice fed a HFD (Fig. 2b). Furthermore, gene expression measurements of HFD-fed mouse hearts showed up-regulation of both ANP and β-MHC mRNA in wild-type mice (Fig. 2c and d), providing further evidence in support of a hypertrophic phenotype. Consistently, both ANP and β-MHC mRNA expression were not increased in *capns1-ko* mice fed a HFD compared with a ND (Fig. 2c and d). There were no differences in cardiomyocyte size and hypertrophic gene expression when comparing *capns1-ko* mice and their wild-type littermates fed a ND (Fig. 2b–d). These results demonstrate that *capns1* knockout prevents HFD-induced myocardial hypertrophy.

3.4. Deletion of capns1 inhibits myocardial fibrosis in mice fed a HFD

To determine cardiac fibrosis, myocardial tissues were stained with picrosirius red to highlight collagen. Deposition of total collagen was increased in HFD-fed mouse hearts as determined by the ratio of collagen area to total area; however, *capns1* deletion correlated with a significant reduction in those levels in *capns1-ko* mice fed a HFD (Fig. 3a and b). Polarization microscopic analysis revealed an increase in both collagen type-1 and -3

depositions in HFD-fed mouse hearts, which was attenuated by *capns1* knockout (Fig. 3a, c and d). Similar to altered deposition of collagen-1 and -3, deletion of *capns1* lowered the mRNA levels of collagen-1 and -3 in HFD-fed *capns1-ko* mouse hearts (Fig. 3e and f). Thus, disruption of calpain prevented myocardial fibrosis in mice fed a HFD.

3.5. Knockout of calpain prevents ER stress, caspase-12 and caspase-3 activation, and pro-inflammatory cytokine expression in mice fed a HFD

To gain insights into the role of calpain, we examined ER stress and caspase-12 activation in cardiac lipotoxicity. HFD induced caspase-12 cleavage (Fig. 4a) and elevated the protein levels of GRP78, CHOP and phosphorylated JNK1/2 in heart tissues, indicative of ER stress (Fig. 4b–d). Deletion of *capns1* decreased the protein levels of cleaved caspase-12, GRP78, CHOP and phosphorylated JNK1/2 in HFD-fed mouse hearts, but did not change their levels in normal diet-fed mouse hearts (Supplemental Fig. 3a), suggesting an important role of calpain in lipotoxicity-induced ER stress.

To investigate the linking between calpain and ER stress, we examined the protein levels of SERCA2a [18], STIM1 [19] and junctophilin-2 [20], previously reported as targets of calpain. HFD induced a reduction in junctophilin-2 protein levels (Fig. 4e and f) but not SERCA2a and STIM1 in hearts (data not shown). Deletion of *capns1* restored the protein levels of junctophilin-2 in HFD-fed mouse hearts. This result suggests that junctophilin-2 is a substrate of calpain in HFD-fed mouse hearts.

Since ER stress mediates apoptosis in cardiomyocytes, we determined caspase-3 activity in the heart. As shown in Fig. 5a, caspase-3 activity was increased in hearts of mice fed a HFD versus ND, which was abrogated by *capns1* knockout. ER stress has also been implicated in pro-inflammatory response. Consistently, the mRNA levels of pro-inflammatory cytokines TNF-α and IL-1β were elevated in HFD-fed mouse hearts. In line with inhibition of ER stress, deletion of *capns1* significantly decreased the mRNA levels of TNF-α and IL-1β in HFD-fed *capns1-ko* mice compared with their wild-type littermates (Fig. 5b and c). These results suggest that calpain may play a role in ER stress, apoptosis and pro-inflammatory response in cardiac lipotoxicity.

3.6. Role of calpain in ER stress, apoptosis and pro-inflammatory response in cultured cardiomyocytes during high palmitate stimulation

To provide direct evidence to support the role of calpain in cardiomyocytes, we incubated cultured cardiomyocytes with high palmitate or oleate (200 μmol/L) as an osmotic and a diet control in the presence of calpain inhibitor-III (10 μmol/L) or vehicle for 24 h. Incubation with high palmitate elevated calpain activity (Fig. 6a). High palmitate also increased the protein levels of ER stress markers (GRP78, CHOP and phosphorylated JNK1/2) (Fig. 6b and c), and induced apoptosis as determined by an increased in caspase-3 activity and DNA fragmentation in cardiomyocytes (Fig. 6d and e). All these effects of high palmitate were prevented by calpain inhibitor-III. However, calpain inhibitor-III did not change the basal levels of ER stress markers in oleate-treated cardiomyocytes.

To substantiate the role of calpain and determine which isoforms of calpain were involved, we silenced *capn1* and *capn2* in cardiomyocytes using their specific siRNAs, respectively

(Supplemental Fig. 4a and b). Silencing of *capn1* but not *capn2* inhibited palmitate-induced apoptosis and ER stress (Fig. 7a–d and Supplemental Fig. 4c–e), suggesting that calpain-1 activation directly contributes to lipotoxicity-induced injury in cardiomyocytes. We also determined TNF-α and IL-1β expression in cardiomyocytes. High palmitate up-regulated the mRNA levels of TNF-α and IL-1β. However, silencing of *capn1* prevented high palmitate-induced TNF-α and IL-1β mRNA expression (Fig. 7e and f), supporting the causal role of calpain-1 in lipotoxicity-induced pro-inflammatory response in cardiomyocytes.

To further confirm the role of calpain, we incubated adult cardiomyocytes from wild-type and *capns1* knockout mice with oleate or palmitate (200 μmol/L) for 20 h. Palmitate increased cell death in wild-type cardiomyocytes by 58% compared with oleate; however, palmitate-induced cell death was significantly reduced in *capns1* knockout cardiomyocytes (Fig. 8a and b).

3.7. Effects of ER stress inhibitor on apoptosis and pro-inflammatory response in cultured cardiomyocytes during high palmitate stimulation

To determine the role of ER stress in apoptosis and pro-inflammatory response, we incubated cultured cardiomyocytes with high palmitate or oleate (200 μmol/L) as an osmotic and a diet control in the presence of ER stress inhibitor, tauroursodeoxycholate (TAUR, 100 μmol/L) or vehicle for 24 h. Consistently, high palmitate induced caspase-3 activity and DNA fragmentation (Fig. 8c and d), and up-regulated the mRNA levels of TNF-α and IL-1β in cardiomyocytes (Fig. 8e and f), all of which were prevented by TAUR. This result indicates that ER stress mediates apoptosis and proinflammatory response in lipotoxicity.

4. Discussion

Both lipotoxicity and glucotoxicity are important mechanisms contributing to diabetic cardiomyopathy. We have recently demonstrated that calpain activation plays a critical role in cardiac glucotoxicity [5, 7]; however, its pathophysiological significance in cardiac lipotoxicity remains to be determined. In the present study, we demonstrated that disruption of calpain prevented lipotoxicity-induced cardiac injury by inhibiting ER stress and subsequent apoptosis and pro-inflammatory response, leading to the improvement of myocardial function. Thus, this study provides significant insights into and new therapeutic targets for cardiac lipotoxicity.

Calpain is activated in cardiomyocytes during hyperglycemia [5,7]. It was reported that incubation of saturated fatty acid induces Ca^{2+} dysregulation in cardiomyocytes [21]. Since Ca^{2+} dysregulation or dyshomeostasis is implicated in calpain activation, we showed that incubation with palmitate increased calpain activity in cardiomyocytes and calpain activity was elevated in HFD-fed mouse hearts while the protein levels of CAPN1, CAPN2 and calpastatin remained unchanged, suggesting that lipotoxicity activates calpain in cardiomyocytes. The activation of calpain contributes to cardiac injury and heart failure [6]. In this study, cardiomyocyte-specific deletion of *capns1* reduced myocardial caspase-3 activity, hypertrophy and fibrosis in mice fed a HFD, resulting in attenuation of myocardial dysfunction, indicating that calpain activation mediates lipotoxicity-induced cardiac injury.

Cardiac-specific disruption of calpain did not influence systemic metabolic disorder in mice fed a HFD. Thus, the attenuation of cardiac injury directly results from calpain disruption in cardiomyocytes. However, blood glucose tolerance was impaired in wild-type mice fed a HFD but not in *capns1* knockout mice fed a HFD. This raises a possibility that *capns1* knockout-mediated cardiac protection may be also due to the deregulation of glucose metabolism in the heart, which needs further study for clarification. Nevertheless, the direct role of calpain in cardiac lipotoxicity was supported by observations in cultured cardiomyocytes where inhibition of calpain prevented palmitate-induced apoptotic cell death. The anti-apoptotic effect of calpain inhibition was further confirmed by *capn1* siRNA in palmitate-stimulated cardiomyocytes and using adult *capns1* knockout cardiomyocytes, suggesting that calpain-1 contributes to lipotoxicity-induced cardiac injury. The pro-apoptotic role of calpain-1 has also been demonstrated in cardiomyocytes under other pathological conditions, such as hypoxia/re-oxygenation [14] and hyperglycemia [7]. Given that over-expression of CAPN2 did not induce apoptosis in cardiomyocytes [14], this study showed that silencing of *capn2* had no effect on palmitate-stimulated apoptosis in cardiomyocytes, suggesting that calpain-2 may play no role in cardiac lipotoxicity. It is important to point out there is no information on the calorie taken from normal diet and HFD by wild-type and *capns1* knockout mice. In the future, the calorie matching needs to be considered if possible.

Multiple mechanisms have been proposed to be responsible for cardiac lipotoxicity. Several lipid species have been implicated in cardiac lipotoxicity: fatty acid/fatty acyl CoA, acylcarnitine, unesterified cholesterol, lysolecithin, ceramide, and diacylglycerol [17]. We showed that HFD increased the content of triglyceride in the heart. Accumulation of these toxic lipid species is associated with apoptosis [22] and ER stress [12,13]. We have recently reported that caplain-1 activation sufficiently induces ER stress in cardiomyocytes [14]. Thus, the present study examined whether ER stress is a potential mechanism underlying calpain-mediated cardiac lipotoxicity. We demonstrated that ER stress was induced in HFD-fed mouse hearts. More importantly, we showed for the first time that calpain deficiency inhibited the expression of ER stress markers in lipotoxic hearts, suggesting a critical role of calpain activation in ER stress. To characterize whether the role of calpain in ER stress could be reproduced by high palmitate, we extended our analyses to cultured cardiomyocytes. Direct exposure of cardiomyocytes to high palmitate induced ER stress. Selective inhibition of calpain by pharmacological inhibitor or silencing of *capn1* prevented ER stress in high palmitate-stimulated cardiomyocytes. Taken together, ER stress may represent an important mechanism by which calpain-1 contributes to lipotoxic cardiac injury. It is currently unknown how calpain-1mediates ER stress in cardiac lipotoxicity. Our data suggest that a reduction of junctophilin-2 protein may link calpain-1 to ER stress because decreased junctophilin-2 disrupts t-tubule system [23] and impairs ryanodine receptor-2 stability [24]. Abnormal t-tubule results in Ca^{2+} mishandling, and loss of ryanodine receptor-2 stability increases Ca^{2+} leak from sarco/endoplasmic reticulum, both of which contribute to ER stress. However, this merits future investigation.

Although calpain-2 has been implicated in ER stress in neuronal cells [25] and fibroblasts [26], the present study did not support a role of calpain-2 in ER stress in cardiomyocytes upon palmitate stimulation. However, it is worthwhile to mention that siRNA only partially

remove CAPN2 protein expression in cardiomyocytes and thus, complete knockout of *capn2* may be useful to clarify the role of calpain-2 in palmitate-induced ER stress in cardiomyocytes. Furthermore, the *in vivo* role of calpain-2 needs to be determined using capn2 knockout mice.

It is well known that ER stress induces apoptosis in cardiomyocytes [27]. In this regard, we showed that incubation with ER stress inhibitor protected cardiomyocytes against palmitate-induced apoptosis. In addition to apoptosis, ER stress has been implicated in cardiac hypertrophy [28] and heart failure [27]. Thus, ER stress may be one of important mechanisms by which calpain activation mediates cardiac injury in response to lipotoxicity.

A cross-talk between ER stress, mitogen activated protein kinases (e.g. p38 and JNK1/2) signaling [29] and NF-κB activation [30] has been associated with pro-inflammatory response. It has been reported that incubation with saturated long-chain fatty acids promotes pro-inflammatory response in human coronary artery endothelial cells [31], human pancreatic islets [32] and rat insulinoma cell line [33]. In this study, we observed up-regulation of TNF-α and IL-1β expression in palmitate-stimulated cardiomyocytes and HFD-fed mouse hearts. Inhibition of ER stress prevented TNF-α and IL-1β expression in palmitate-stimulated cardiomyocytes, confirming the role of ER stress in lipotoxicity-induced pro-inflammatory response. It is known that excessive expression of pro-inflammatory cytokines is detrimental to cardiomyocytes. For example, TNF-α disrupts Ca^{2+} influx through L-type Ca^{2+} channels and Ca^{2+}-induced Ca^{2+} release from the sarcoplas-mic reticulum [34]. In addition to Ca^{2+} dyshomeostasis, TNF-α also causes direct cytotoxicity [35], oxidative stress [36], disruption of excitation-contraction coupling [37], up-regulation of other cardiac suppressing cytokines (e.g., IL-1β) [38,39] and induction of cardiomyocyte apoptosis [40], all of which impair cardiac contractile function in cardiomyocytes, isolated hearts and intact animals. Pro-inflammatory response may also promote fibrosis in heart [41,42]. Having shown that disruption of calpain inhibited ER stress, we further demonstrated that deletion of *capns1* prevented pro-inflammatory cytokines expression in HFD-fed mouse hearts and silencing of *capn1* inhibited palmitate-induced pro-inflammatory response in cardiomyocytes. Thus, calpain/ER stress-mediated pro-inflammatory response may be a potential mechanism underlying cardiac lipotoxicity.

5. Conclusion

The present study has demonstrated that inhibition of calpain prevents palmitate-induced apoptosis in cardiomyocytes, reduces hypertrophy and fibrosis, and preserves myocardial function in a mouse model of HFD-induced cardiac lipotoxicity. These protective effects of calpain inhibition may be mediated, at least partly, by preventing ER stress. Taken together with our recent findings that calpain activation significantly contributes to cardiac glucotoxicity [5, 7], calpain may represent an important therapeutic target for diabetic cardiac complications.

Supplementary Material

Refer to Web version on PubMed Central for supplementary material.

Acknowledgments

This work was supported by operating grants from the National Natural Science Foundation of China [81470499], Program for Changjiang Scholars and Innovative Research Team in University (PCSIRT, IRT1075) and the Canadian Institutes of Health Research [MOP-133657].

References

1. Alpert MA. Obesity cardiomyopathy: pathophysiology and evolution of the clinical syndrome. Am J Med Sci. 2001; 321:225–236. [PubMed: 11307864]
2. Goldberg IJ, Trent CM, Schulze PC. Lipid metabolism and toxicity in the heart. Cell Metab. 2012; 15:805–812. [PubMed: 22682221]
3. Bayeva M, Sawicki KT, Ardehali H. Taking diabetes to heart—deregulation of myocardial lipid metabolism in diabetic cardiomyopathy. J Am Heart Assoc. 2013; 2:e000433. [PubMed: 24275630]
4. Goll DE, Thompson VF, Li H, Wei W, Cong J. The calpain system. Physiol Rev. 2003; 83:731–801. [PubMed: 12843408]
5. Li Y, Ma J, Zhu H, Singh M, Hill D, Greer PA, Arnold JM, Abel ED, Peng T. Targeted inhibition of calpain reduces myocardial hypertrophy and fibrosis in mouse models of type 1 diabetes. Diabetes. 2011; 60:2985–2994. [PubMed: 21911754]
6. Letavernier E, Zafrani L, Perez J, Letavernier B, Haymann JP, Baud L. The role of calpains in myocardial remodelling and heart failure. Cardiovasc Res. 2012; 96:38–45. [PubMed: 22425901]
7. Li Y, Li Y, Feng Q, Arnold M, Peng T. Calpain activation contributes to hyperglycaemia-induced apoptosis in cardiomyocytes. Cardiovasc Res. 2009; 84:100–110. [PubMed: 19505932]
8. Claudio H. The unfolded protein response: controlling cell fate decisions under ER stress and beyond. Nat Rev Mol Cell Biol. 2012; 13:89–102. [PubMed: 22251901]
9. Tetsuo M, Masafumi K. ER stress in cardiovascular disease. J Mol Cell Cardiol. 2010; 48:1105–1110. [PubMed: 19913545]
10. Sozen E, Karademir B, Ozer NK. Basic mechanisms in endoplasmic reticulum stress and relation to cardiovascular diseases. Free Radic Biol Med. 2015; 78:30–41. [PubMed: 25452144]
11. Borradaile NM, Buhman KK, Listenberger LL, Magee CJ, Morimoto ET, Ory DS, Schaffer JE. A critical role for eukaryotic elongation factor 1A-1 in lipotoxic cell death. Mol Biol Cell. 2006; 17:770–778. [PubMed: 16319173]
12. Bosma M, Dapito DH, Drosatos-Tampakaki Z, Huiping-Son N, Huang LS, Kersten S, Drosatos K, Goldberg IJ. Sequestration of fatty acids in triglycerides prevents endoplasmic reticulum stress in an in vitro model of cardiomyocyte lipotoxicity. Biochim Biophys Acta. 2014; 1841:1648–1655. [PubMed: 25251292]
13. Park M, Sabetski A, Kwan Chan Y, Turdi S, Sweeney G. Palmitate induces ER stress and autophagy in H9c2 cells: implications for apoptosis and adiponectin resistance. J Cell Physiol. 2015; 230:630–639. [PubMed: 25164368]
14. Zheng D, Wang G, Li S, Fan GC, Peng T. Calpain-1 induces endoplasmic reticulum stress in promoting cardiomyocyte apoptosis following hypoxia/reoxygenation. Biochim Biophys Acta. 2015; 1852:882–892. [PubMed: 25660447]
15. Wang Y, Zheng D, Wei M, Ma J, Yu Y, Chen R, Lacefield JC, Xu H, Peng T. Over-expression of calpastatin aggravates cardiotoxicity induced by doxorubicin. Cardiovasc Res. 2013; 98:381–390. [PubMed: 23455548]
16. Zheng D, Ma J, Yu Y, Li M, Ni R, Wang G, Chen R, Li J, Fan GC, Lacefield JC, Peng T. Silencing of miR-195 reduces diabetic cardiomyopathy in C57BL/6 mice. Diabetologia. 2015; 58:1949–1958. [PubMed: 25994075]
17. Drosatos K, Schulze PC. Cardiac lipotoxicity: molecular pathways and therapeutic implications. Curr Heart Fail Rep. 2013; 10:109–121. [PubMed: 23508767]
18. French JP, Quindry JC, Falk DJ, Staib JL, Lee Y, Wang KK, Powers SK. Ischemia-reperfusion-induced calpain activation and SERCA2a degradation are attenuated by exercise training and calpain inhibition. Am J Physiol Heart Circ Physiol. 2006; 290:H128–H136. [PubMed: 16155100]

19. Prins D, Michalak M. STIM1 is cleaved by calpain. FEBS Lett. 2015; 589:3294–3301. [PubMed: 26454179]
20. Guo A, Hall D, Zhang C, Peng T, Miller JD, Kutschke W, Grueter CE, Johnson FL, Lin RZ, Song LS. Molecular determinants of calpain-dependent cleavage of junctophilin-2 protein in cardiomyocytes. J Biol Chem. 2015; 290:17946–17955. [PubMed: 26063807]
21. Haim TE, Wang W, Flagg TP, Tones MA, Bahinski A, Numann RE, Nichols CG, Nerbonne JM. Palmitate attenuates myocardial contractility through augmentation of repolarizing Kv currents. J Mol Cell Cardiol. 2010; 48:395–405. [PubMed: 19857498]
22. Zhu H, Yang Y, Wang Y, Li J, Schiller PW, Peng T. MicroRNA-195 promotes palmitate-induced apoptosis in cardiomyocytes by down-regulating Sirt1. Cardiovasc Res. 2011; 92:75–84. [PubMed: 21622680]
23. Guo A, Zhang C, Wei S, Chen B, Song LS. Emerging mechanisms of T-tubule remodelling in heart failure. Cardiovasc Res. 2013; 98:204–215. [PubMed: 23393229]
24. Wang W, Landstrom AP, Wang Q, Munro ML, Beavers D, Ackerman MJ, Soeller C, Wehrens XH. Reduced junctional Na^{+}/Ca^{2+}-exchanger activity contributes to sarcoplasmic reticulum Ca^{2+} leak in junctophilin-2-deficient mice. Am J Physiol Heart Circ Physiol. 2014; 307:H1317–H1326. [PubMed: 25193470]
25. Lu S, Kanekura K, Hara T, Mahadevan J, Spears LD, Oslowski CM, Martinez R, Yamazaki-Inoue M, Toyoda M, Neilson A, Blanner P, Brown CM, Semenkovich CF, Marshall BA, Hershey T, Umezawa A, Greer PA, Urano F. A calcium-dependent protease as a potential therapeutic target for Wolfram syndrome. Proc Natl Acad Sci U S A. 2014; 111:E5292–E5301. [PubMed: 25422446]
26. Tan Y, Dourdin N, Wu C, De Veyra T, Elce JS, Greer PA. Ubiquitous calpains promote caspase-12 and JNK activation during endoplasmic reticulum stress-induced apoptosis. J Biol Chem. 2006; 281:16016–16024. [PubMed: 16597616]
27. Wang J, Hu X, Jiang H. ER stress-induced apoptosis: a novel therapeutic target in heart failure. Int J Cardiol. 2014; 177:564–565. [PubMed: 25179556]
28. Zhang ZY, Liu XH, Ye YJ, Sun S, Rong F, Guo XS, Hu WC. C/EBP homologous protein-mediated endoplasmic reticulum stress-related apoptosis pathway is involved in abdominal aortic constriction-induced myocardium hypertrophy in rats. Sheng Li Xue Bao (Acta Physiol Sin). 2009; 61:161–168.
29. Wei SG, Yu Y, Weiss RM, Felder RB. Inhibition of brain mitogen-activated protein kinase signaling reduces central endoplasmic reticulum stress and inflammation and sympathetic nerve activity in heart failure rats. Hypertension. 2016; 67:229–236. [PubMed: 26573710]
30. Rao J, Yue S, Fu Y, Zhu J, Wang X, Busuttil RW, Kupiec-Weglinski JW, Lu L, Zhai Y. ATF6 mediates a pro-inflammatory synergy between ER stress and TLR activation in the pathogenesis of liver ischemia-reperfusion injury. Am J Transplant. 2014; 14:1552–1561. [PubMed: 24903305]
31. Harvey KA, Walker CL, Pavlina TM, Xu Z, Zaloga GP, Siddiqui RA. Long-chain saturated fatty acids induce pro-inflammatory responses and impact endothelial cell growth. Clin Nutr. 2010; 29:492–500. [PubMed: 19926177]
32. Igoillo-Esteve M, Marselli L, Cunha DA, Ladriere L, Ortis F, Grieco FA, Dotta F, Weir GC, Marchetti P, Eizirik DL, Cnop M. Palmitate induces a pro-inflammatory response in human pancreatic islets that mimics CCL2 expression by beta cells in type 2 diabetes. Diabetologia. 2010; 53:1395–1405. [PubMed: 20369226]
33. Li S, Du L, Zhang L, Hu Y, Xia W, Wu J, Zhu J, Chen L, Zhu F, Li C, Yang S. Cathepsin B contributes to autophagy-related 7 (Atg7)-induced nod-like receptor 3 (NLRP3)-dependent proinflammatory response and aggravates lipotoxicity in rat insulinoma cell line. J Biol Chem. 2013; 288:30094–30104. [PubMed: 23986436]
34. Duncan DJ, Yang Z, Hopkins PM, Steele DS, Harrison SM. TNF-alpha and IL-1beta increase Ca^{2+} leak from the sarcoplasmic reticulum and susceptibility to arrhythmia in rat ventricular myocytes. Cell Calcium. 2010; 47:378–386. [PubMed: 20227109]
35. Kewalramani G, Puthanveetil P, Wang F, Kim MS, Deppe S, Abrahani A, Luciani DS, Johnson JD, Rodrigues B. AMP-activated protein kinase confers protection against TNF-{alpha}-induced cardiac cell death. Cardiovasc Res. 2009; 84:42–53. [PubMed: 19477967]

36. Suzuki H, Kayama Y, Sakamoto M, Iuchi H, Shimizu I, Yoshino T, Katoh D, Nagoshi T, Tojo K, Minamino T, Yoshimura M, Utsunomiya K. Arachidonate 12/15-lipoxygenase-induced inflammation and oxidative stress are involved in the development of diabetic cardiomyopathy. Diabetes. 2015; 64:618–630. [PubMed: 25187369]
37. Hobai IA, Morse JC, Siwik DA, Colucci WS. Lipopolysaccharide and cytokines inhibit rat cardiomyocyte contractility in vitro. J Surg Res. 2015; 193:888–901. [PubMed: 25439505]
38. Di Bartolo BA, Chan J, Bennett MR, Cartland S, Bao S, Tuch BE, Kavurma MM. TNF-related apoptosis-inducing ligand (TRAIL) protects against diabetes and atherosclerosis in Apoe$^{-/-}$ mice. Diabetologia. 2011; 54:3157–3167. [PubMed: 21965021]
39. Yoshida T, Friehs I, Mummidi S, del Nido PJ, Addulnour-Nakhoul S, Delafontaine P, Valente AJ, Chandrasekar B. Pressure overload induces IL-18 and IL-18R expression, but markedly suppresses IL-18BP expression in a rabbit model. IL-18 potentiates TNF-alpha-induced cardiomyocyte death. J Mol Cell Cardiol. 2014; 75:141–151. [PubMed: 25108227]
40. Yan L, Tang Q, Shen D, Peng S, Zheng Q, Guo H, Jiang M, Deng W. SOCS-1 inhibits TNF-alpha-induced cardiomyocyte apoptosis via ERK1/2 pathway activation. Inflammation. 2008; 31:180–188. [PubMed: 18330685]
41. Shinde AV, Frangogiannis NG. Fibroblasts in myocardial infarction: a role in inflammation and repair. J Mol Cell Cardiol. 2014; 70:74–82. [PubMed: 24321195]
42. Turner NA. Inflammatory and fibrotic responses of cardiac fibroblasts to myocardial damage associated molecular patterns (DAMPs). J Mol Cell Cardiol. 2015 doi:30110.31016/j.yjmcc.32015.30111.30002. Epub ahead of print.

Abbreviations

ANP	atrial natriuretic peptide
ATF4	activating transcription factor 4
β-MHC	beta-myosin heavy chain
capns1	small regulatory subunit of calpain
CHOP	C/EBP homologous protein
ER	endoplasmic reticulum
GRP78	chaperones glucose-regulated protein-78
GRP94	chaperones glucose-regulated protein-94
HDL-C	high-density lipoprotein cholesterol
HFD	high fat diet
IL-1β	interleukin-1 beta
IPGTT	intra-peritoneal glucose tolerance test
LDL-C	low-density lipoprotein cholesterol
LV	left ventricle
ND	normal diet
TC	total cholesterol

TG	triglyceride
TNF-α	tumor necrosis factor-alpha

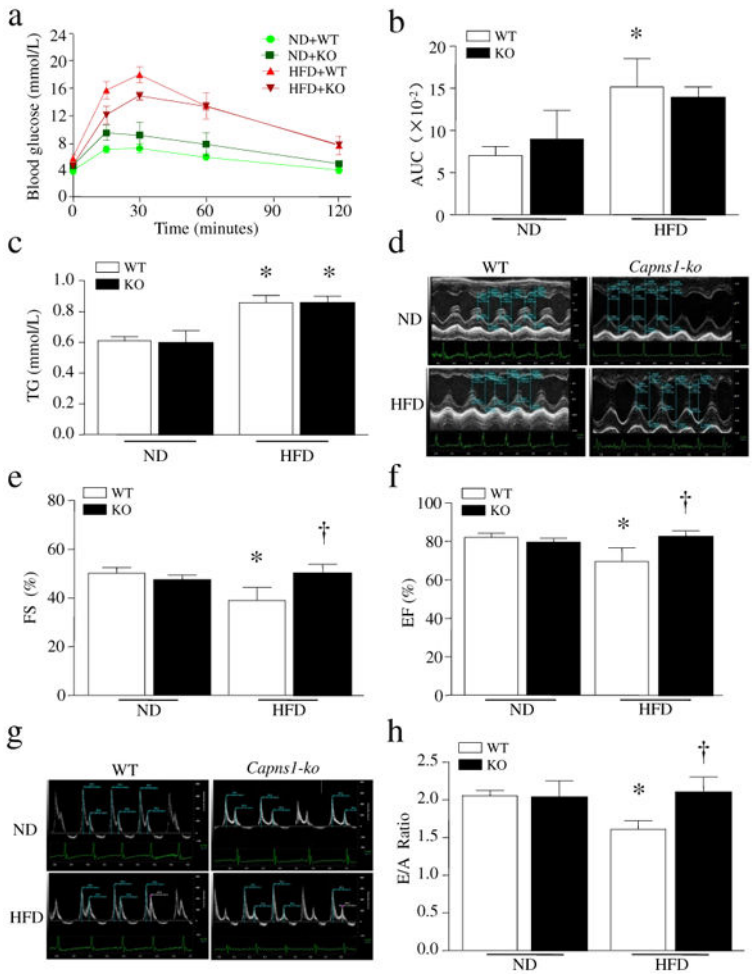

Fig. 1.

Metabolic parameters, triglyceride content and myocardial function. *Capns1*-ko and their wild-type littermates (WT) were fed a HFD or ND for 20 weeks. (a) Glucose tolerance test. (b) Quantification of glucose tolerance. (c) The content of triglyceride was measured in ND- and HFD-fed mouse hearts. (d) A representative view at the papillary muscle level of echocardiography (M-model). (e) Ejection fraction (EF%) and (f) fractional shortening (FS%). (g) A representative mitral E/A ratio on Doppler echocardiography. (h) The E/A ratio. Data are mean ± SD, n = 6–10 per group. $^{*}P < 0.05$ *vs* ND + WT and $^{\dagger}P < 0.05$ *vs* HFD + WT.

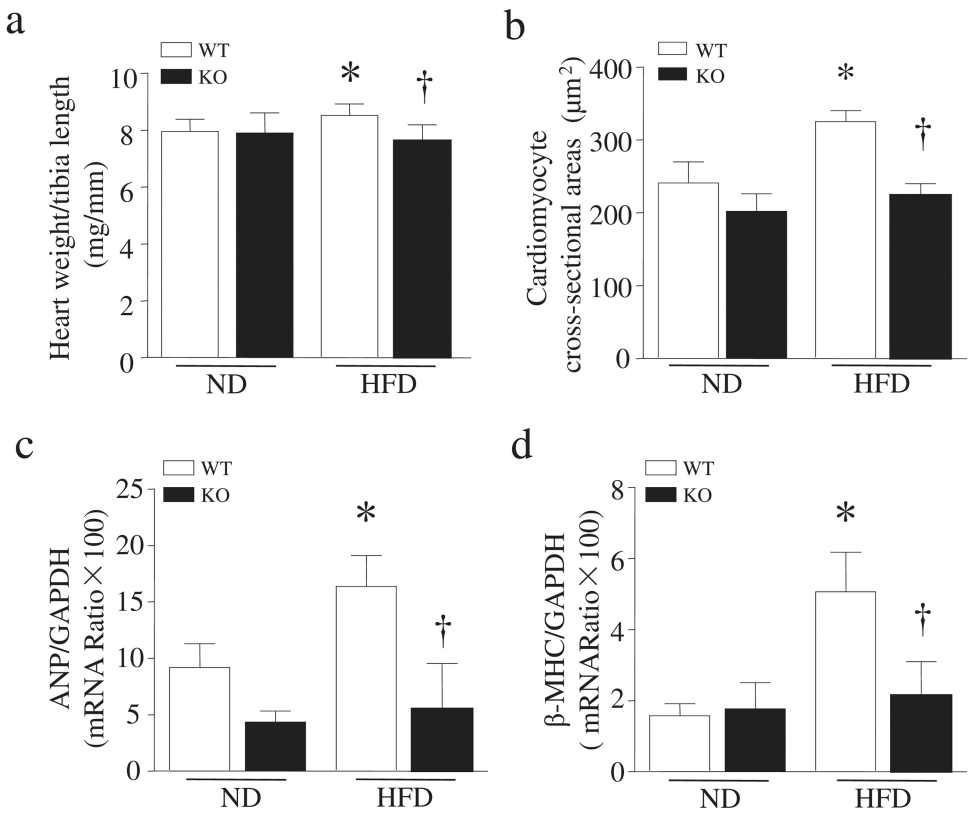

Fig. 2.

Assessment of cardiac hypertrophy. (a) The ratio of heart weight to tibia length. (b) Cardiomyocyte cross-sectional areas. (c) The mRNA levels of ANP and (d) the mRNA levels of β-MHC. Data are mean ± SD, n = 6–8. $^{*}P < 0.05$ *vs* ND + WT and $^{\dagger}P < 0.05$ *vs* HFD + WT.

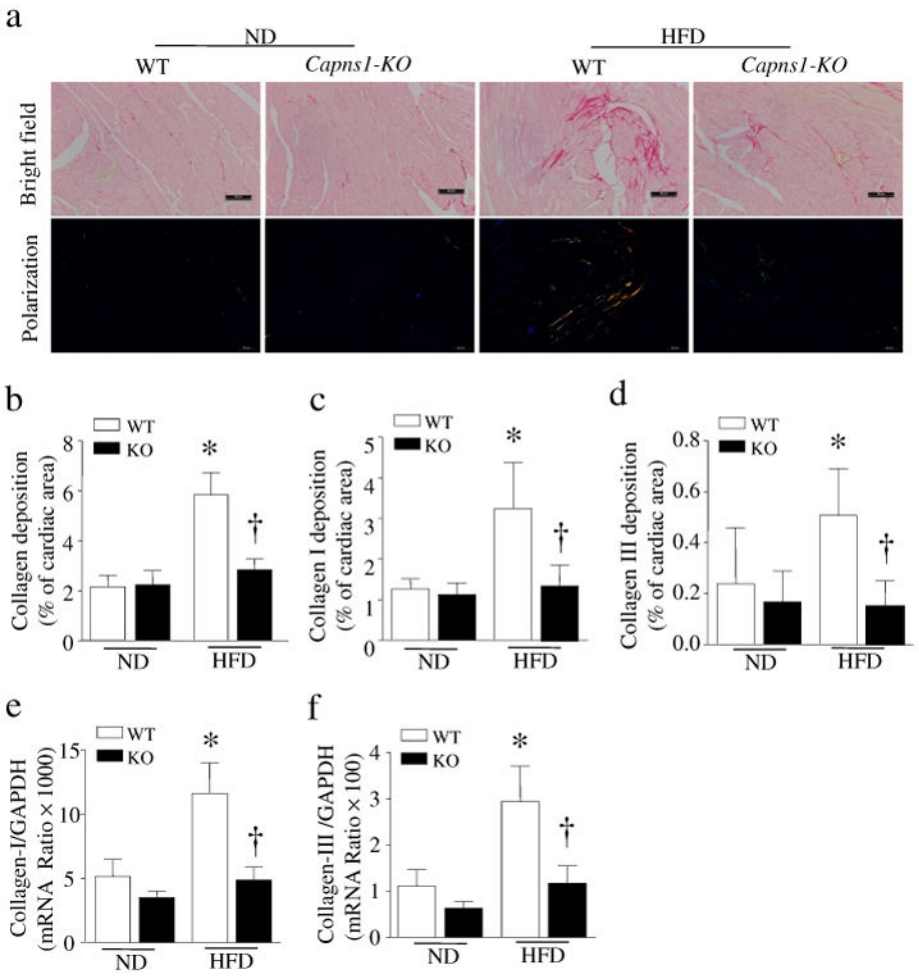

Fig. 3.

Assessment of fibrosis in hearts. (a) Representative Picro-sirius red staining for collagen deposition (red color) and polarization microscopic pictures for collagen-1 (yellow color) and collagen-3 (green color) from *capns1*-ko mice and their wild-type littermates fed a HFD or ND. (b) Total collagen deposition. (c) Collagen-1 deposition. (d) Collagen-3 deposition. The quantification of collagen-1 mRNA (e) and collagen-3 mRNA (f). Data are mean ± SD, n = 6. $^{*}P < 0.05$ *vs* ND + WT and $^{\dagger}P < 0.05$ *vs* HFD + WT.

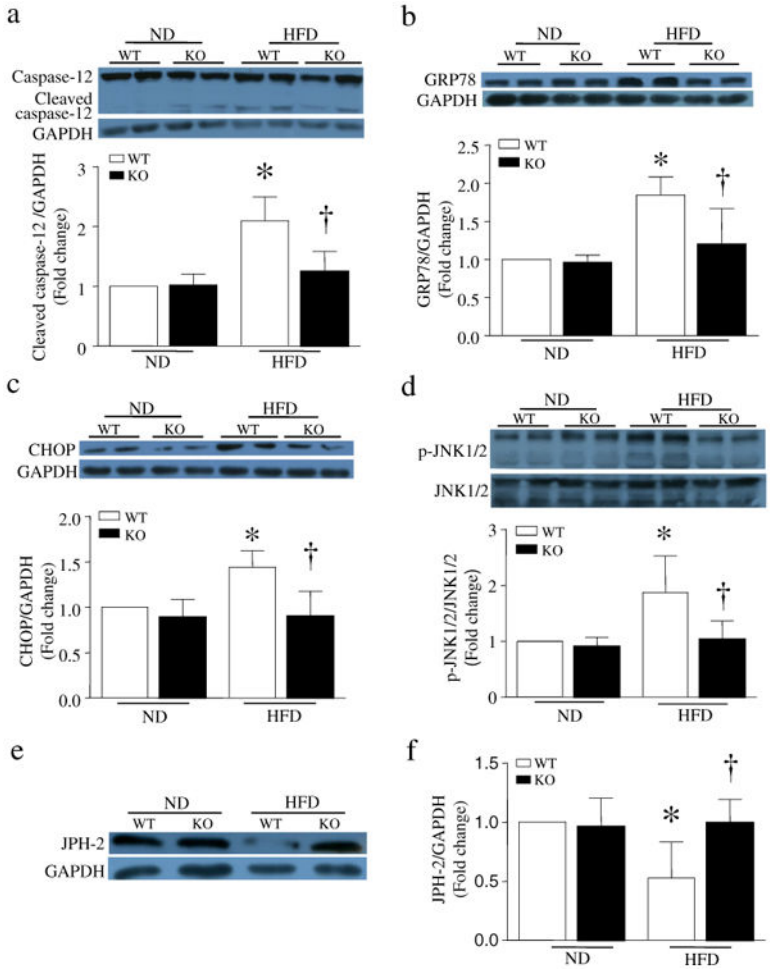

Fig. 4.

Determination of ER stress, caspase-12 cleavage and junctophilin-2 protein inhearts. *Capns1*-ko mice (KO) and their wild-type littermates (WT) were fed a HFD or ND for 20 weeks. The protein levels of caspase-12 and cleaved caspase-12 (a), GRP78 (b), CHOP (c), phosphorylated JNK1/2 (d) and junctophilin-2 (e and f) were measured by using western blot analysis. The upper panel is a representative western blot for 2 out of 6 different hearts in each group and lower panel is the quantification of each protein relative to GAPDH or JNK1/2. Data are mean ± SD, n = 6. $^{*}P < 0.05$ *vs* ND + WT and $^{\dagger}P < 0.05$ *vs* HFD + WT.

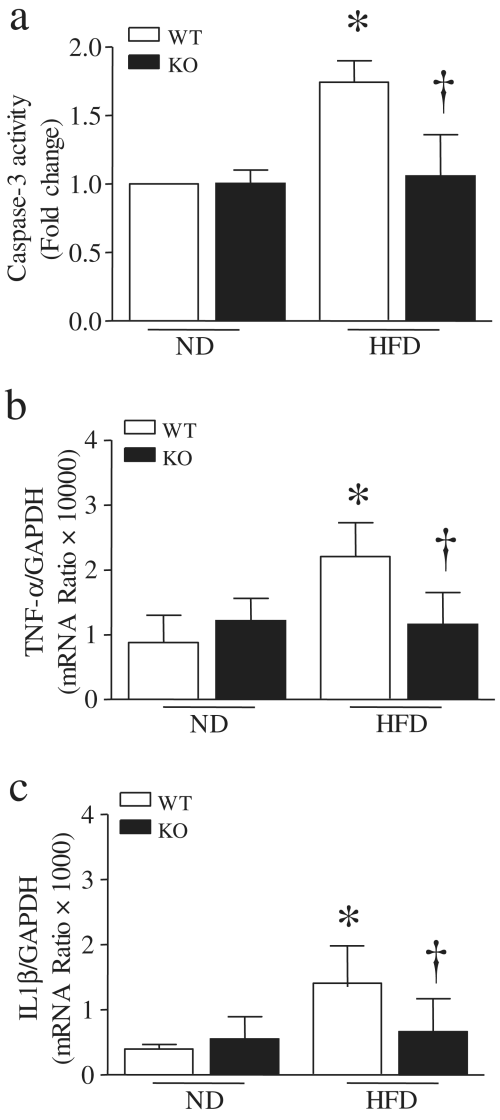

Fig. 5.

Measurement of caspase-3 activity and pro-inflammatory response. *Capns1*-ko mice (KO) and their wild-type littermates (WT) were fed a HFD or ND for 20 weeks. (a) Caspase-3 activity in heart tissues. The mRNA levels of TNF-α (b) and IL-1β (c) were quantified by real-time RT-PCR. Data are mean ± SD, n = 6. $^{*}P < 0.05$ *vs* ND + WT and $^{\dagger}P < 0.05$ *vs* HFD + WT.

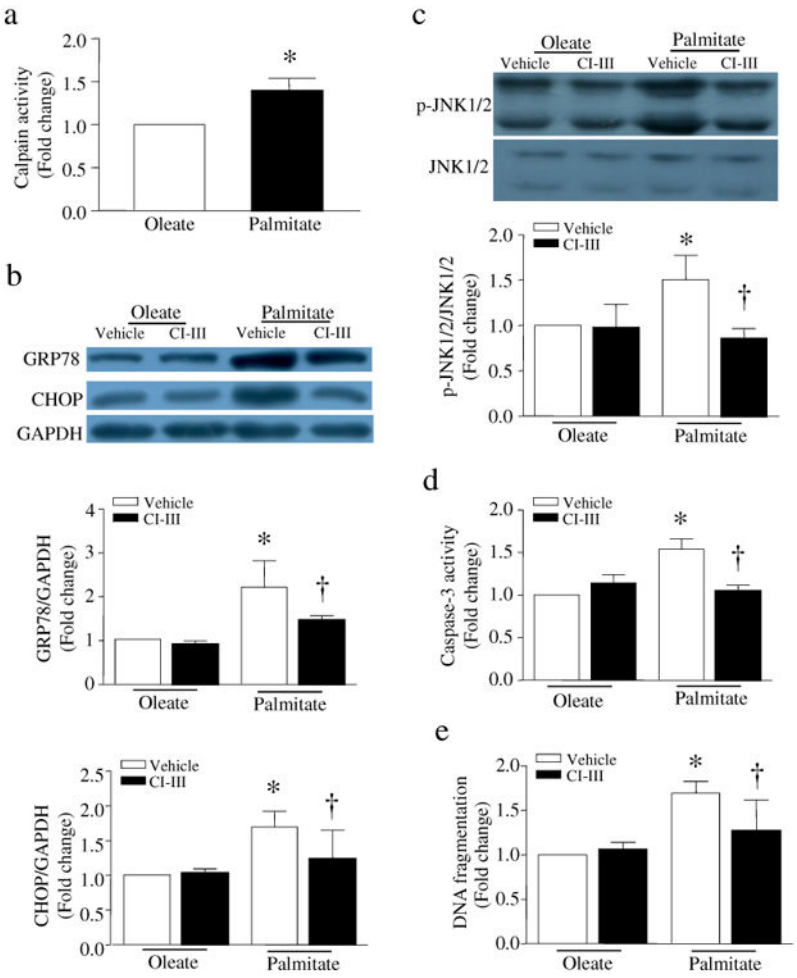

Fig. 6.

Measurement of calpain activity, apoptosis and ER stress. Cultured cardiomyocytes were incubated with high palmitate or oleate inthe presence of calpain inhibitor-IIIor vehicle for 24 h. (a) Calpain activity. (b) The upper panel is a representative western blot for GRP78 and CHOP from at least 3 different cultures, the middle and bottom panel are quantifications of GRP78 and CHOP protein levels relative to GAPDH, respectively. (c) The upper panel is a representative western blot for phosphorylated JNK1/2 and total JNK1/2 from at least 3 different cultures, and the lower panel is the quantification of phosphorylated JNK1/2 protein levels relativeto total JNK1/2. (d) Caspase-3 activity. (e) DNA fragmentation. Data are mean ± SD,n = 4. *$P < 0.05$ *vs* Oleate or Oleate + Vehicle and $^{\dagger}P < 0.05$ *vs* Palmitate + Vehicle.

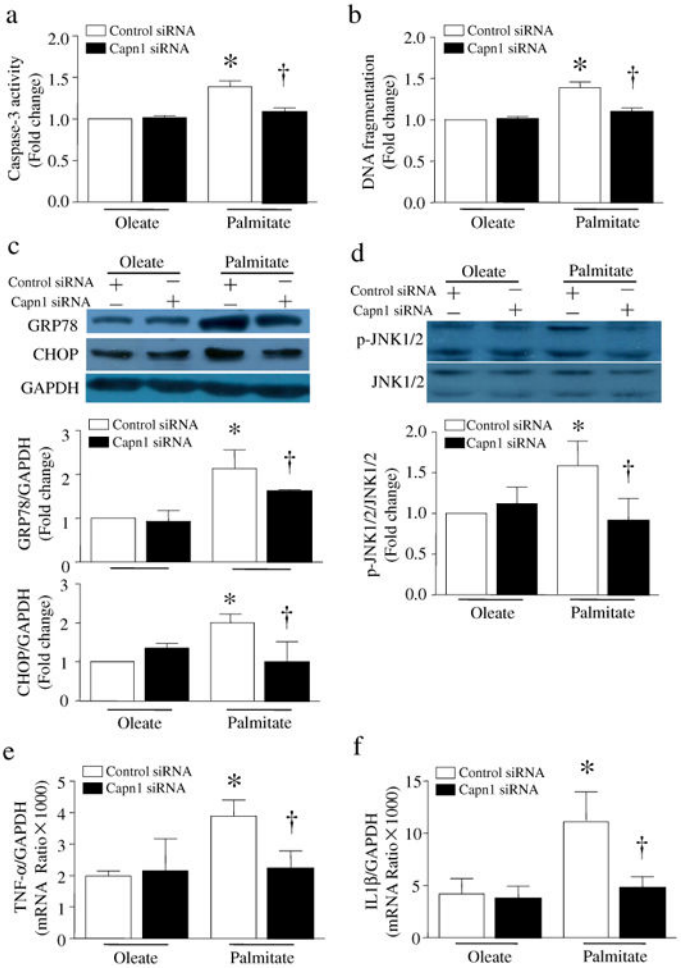

Fig. 7.

Effects of *capn1* silencing on apoptosis, ER stress and pro-inflammatory response. Cultured cardiomyocytes were transfected with *capn1* siRNA or control siRNA, followed by incubation with high palmitate or oleate for 24 h. (a) Caspase-3 activity. (b) DNA fragmentation. (c) The upper panel is a representative western blot for GRP78 and CHOP from at least 3 different cultures, the middle and bottom panel are quantifications of GRP78 and CHOP protein levels relative to GAPDH, respectively. (d) The upper panel is a representative western blot for phosphorylated JNK1/2 and total JNK1/2 from at least 3 different cultures, and the lower panel is the quantification of phosphorylated JNK1/2 protein levels relative to total JNK1/2. The mRNA levels of TNF-α (e) and IL-1β (f) were quantified by real-time RT-PCR. Data are mean ± SD, n = 4. $^{*}P < 0.05$ *vs* Oleate + Control siRNA and $^{\dagger}P < 0.05$ *vs* Control siRNA + Palmitate.

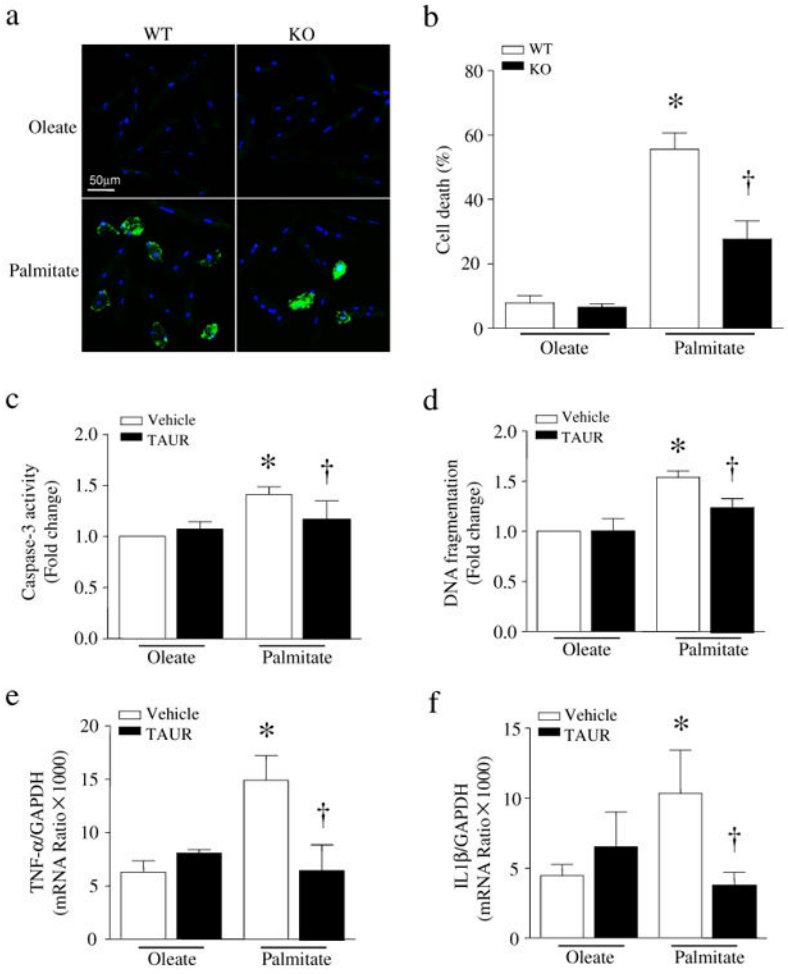

Fig. 8.

Roles of calpain, ER stress in apoptosis and pro-inflammatory response. (a and b) Adult cardiomyocytes were isolated from wild-type (WT) and *capns1* knockout mice (KO), and incubated with high palmitate or oleate for 20 h. Cell death was assessed by annexin V staining (green) and nucleus was stained using Hoechst 33342 (blue). (a) A representative staining for annexin V and (b) quantification of annexin V positive cells from 3 different independent cultures. (c–f) Cultured neonatal cardiomyocytes were incubated with high palmitate or oleate in the presence of ER stress inhibitor TAUR or vehicle for 24 h. (a) Caspase-3 activity. (b) DNA fragmentation. The mRNA levels of TNF-α (c) and IL-1β (d) were quantified by real-time RT-PCR. Data are mean ± SD, n = 4. $^{*}P < 0.05$ *vs* Oleate + Vehicle and $^{\dagger}P < 0.05$ *vs* WT or Vehicle + Palmitate.